

Deterministic Solutions of the Boltzmann Equation for Charge Transport in Graphene on Substrates

Armando Majorana
Department of Mathematics and
Computer Science
University of Catania
Catania, Italy
Email: majorana@dm.unict.it

Giovanni Mascali
Department of Mathematics
University of Calabria and
INFN - Gruppo c. Cosenza, Italy
Email: g.mascali@unical.it

Vittorio Romano
Department of Mathematics and
Computer Science
University of Catania
Catania, Italy
Email: romano@dm.unict.it

Abstract—In this paper, the low and high field mobilities of graphene on substrates are studied, by means of deterministic solutions, obtained using a Discontinuous Galerkin (DG) numerical scheme, of the semiclassical Boltzmann equation for charge transport in graphene. It is shown that there is a strong dependence on the distance between the impurities and the graphene layer with significant changes both in the low and high field mobility curves. We remark that the use of a DG scheme avoids the intrinsic noise typical of the Direct Monte Carlo Simulation (DSMC) results and allows to evaluate the low field mobility with considerable accuracy, making less ambiguous the comparison with experimental measurements.

I. INTRODUCTION

The design of graphene-based electron devices requires an in-deep understanding of the basic transport properties of this material. In realistic situations, the graphene sheet is put over an oxide layer which is the source for additional scatterings between the electrons flowing inside the graphene, and the impurities of the substrate. This remote electron-impurity scattering produces a degradation of the mobility curve (see for example [1], [2]). Therefore in order to develop accurate Computer Aided Design (CAD) tools it is necessary to determine the dependence of the mobility curve on the impurities.

From a modeling point of view several expressions for the dielectric function have been proposed. Here we use the model proposed in [3] which, among several physical parameters, depends in a significant way on the distance between the graphene layer and the impurities inside the oxide. The distance d can vary from zero to few angstroms and depends on the specific specimen one is dealing with.

We want to investigate such a dependence by solving the semiclassical Boltzmann equation for charge transport in graphene including, beside the standard electron-phonon interactions, also the electron-impurity scattering. Solutions of the Boltzmann equations can be obtained with a DSMC approach which of course presents an intrinsic statistical noise, specially at low electric fields. This fact makes it difficult to extract the low field mobility from DSMC results. A promising alternative is to resort to deterministic numerical schemes, like Weighted Essentially Non-Oscillatory (WENO) ones (see [4]). In the present paper, we use the DG method

developed in [5], [6] which gives accurate solutions, so that it is possible to numerically evaluate the low field mobility with good accuracy. For hydrodynamical models, in view of the simulation of graphene based devices, the interested reader is referred to [7], [8].

Besides the parameters discussed above, the dependence on the doping (or equivalently the Fermi energy) must be considered. We will suppose that a gate voltage is applied producing a shift of the Fermi level ε_F in the energy band diagram. Positive Fermi levels will be considered and, therefore, the material behaves as it were n-doped. This situation allows us to neglect the charge transport of the electrons in the valence band. In the meantime tunneling effects around the Dirac point are negligible as well and a semiclassical description is sufficiently accurate from a physical point of view.

The plan of the paper is as follows. In Sect. 2 the transport equation for charge carriers in graphene on substrate is presented. In Sect. 3 the numerical results of charge transport in graphene on SiO₂ are shown and discussed. In particular, the dependence of the mobility curves on the position of the impurities, present in the oxide, is investigated.

II. SEMICLASSICAL MODEL FOR CHARGE TRANSPORT IN GRAPHENE ON A SUBSTRATE

For the purposes to investigate the peculiarities of the charge carrier transport in n-doped graphene, a semiclassical transport model for electrons in the conduction band is considered sufficiently accurate. Since a homogeneous graphene sheet is investigated, spatial dependence is ignored and the model is given by the single Boltzmann equation

$$\frac{\partial f(t, \mathbf{k})}{\partial t} - \frac{e}{\hbar} \mathbf{E} \cdot \nabla_{\mathbf{k}} f(t, \mathbf{k}) = \int S(\mathbf{k}', \mathbf{k}) (1 - f(t, \mathbf{k})) \times f(t, \mathbf{k}') d\mathbf{k}' - \int S(\mathbf{k}, \mathbf{k}') f(t, \mathbf{k}) (1 - f(t, \mathbf{k}')) d\mathbf{k}'. \quad (1)$$

by assuming the K and K' valleys as equivalent. The unknown $f(t, \mathbf{k})$ represents the distribution function of charge carriers at time t and with wave-vector \mathbf{k} . $\nabla_{\mathbf{k}}$ denotes the gradient with respect to the wave-vector. The microscopic velocity \mathbf{v} is related to the energy band ε by

$$\mathbf{v} = \frac{1}{\hbar} \nabla_{\mathbf{k}} \varepsilon.$$

With a very good approximation [9] a linear dispersion relation holds for the energy bands around the equivalent Dirac points; so that $\varepsilon = \hbar v_F |\mathbf{k}|$, where v_F is the (constant) Fermi velocity and \hbar is the Planck constant divided by 2π . The elementary (positive) charge is denoted by e , and \mathbf{E} is the electric field, here assumed to be constant. The right hand side of Eq. (1) is the collision term representing the interaction of electrons with impurities and phonons, the latter due to both the graphene crystal and substrate [10]. Acoustic phonon scattering is intra-valley and intra-band. Phonon scattering with longitudinal and transversal optical phonons (LO and TO , respectively) is intra-valley and can be intra-band or inter-band. Scattering with optical phonons of type K pushes electrons from a valley to the other one (inter-valley scattering). In addition to the interactions already present in the suspended case, surface optical phonon scattering and charged impurity (imp) scattering induced by the substrate are also included. Here, the substrate considered is SiO_2 . Phonons are assumed to be at thermal equilibrium and described by a Bose-Einstein distribution for each branch.

The kernel of the collision operator is the transition rate $S(\mathbf{k}', \mathbf{k})$, which is given by the sum of terms of the kind

$$\left| G^{(\nu)}(\mathbf{k}', \mathbf{k}) \right|^2 \left[\left(n_{\mathbf{q}}^{(\nu)} + 1 \right) \delta \left(\varepsilon(\mathbf{k}) - \varepsilon(\mathbf{k}') + \hbar \omega_{\mathbf{q}}^{(\nu)} \right) + n_{\mathbf{q}}^{(\nu)} \delta \left(\varepsilon(\mathbf{k}) - \varepsilon(\mathbf{k}') - \hbar \omega_{\mathbf{q}}^{(\nu)} \right) \right], \quad (2)$$

related to electron-phonon scatterings and other terms corresponding to the scatterings with the impurities. The index ν labels the ν th phonon mode, $G^{(\nu)}(\mathbf{k}', \mathbf{k})$ is the scattering matrix, which describes the scattering mechanism, due to phonons ν . The symbol δ denotes the Dirac distribution, $\omega_{\mathbf{q}}^{(\nu)}$ is the ν th constant phonon frequency, $n_{\mathbf{q}}^{(\nu)}$ is the Bose-Einstein distribution for the phonon of type ν ,

$$n_{\mathbf{q}}^{(\nu)} = \frac{1}{e^{\hbar \omega_{\mathbf{q}}^{(\nu)} / k_B T} - 1},$$

k_B is the Boltzmann constant and T the constant graphene lattice temperature. The expressions of the electron-phonon scattering matrices used in our simulations are as follows.

For acoustic phonons, we consider the elastic approximation

$$\left(2 n_{\mathbf{q}}^{(ac)} + 1 \right) \left| G^{(ac)}(\mathbf{k}', \mathbf{k}) \right|^2 = \frac{1}{(2\pi)^2} \frac{\pi D_{ac}^2 k_B T}{2\hbar \sigma_m v_p^2} (1 + \cos \vartheta_{\mathbf{k}, \mathbf{k}'}), \quad (3)$$

where D_{ac} is the acoustic phonon coupling constant, v_p is the sound speed in graphene, σ_m the graphene areal density, and $\vartheta_{\mathbf{k}, \mathbf{k}'}$ is the convex angle between \mathbf{k} and \mathbf{k}' .

As said, there are three relevant optical phonon scatterings, the longitudinal optical (LO) and the transversal optical (TO), and the K phonons. The relative scattering matrices are

$$\left| G^{(LO)}(\mathbf{k}', \mathbf{k}) \right|^2 = \frac{1}{(2\pi)^2} \frac{\pi D_O^2}{\sigma_m \omega_O} (1 - \cos \varphi) \quad (4)$$

$$\left| G^{(TO)}(\mathbf{k}', \mathbf{k}) \right|^2 = \frac{1}{(2\pi)^2} \frac{\pi D_O^2}{\sigma_m \omega_O} (1 + \cos \varphi) \quad (5)$$

$$\left| G^{(K)}(\mathbf{k}', \mathbf{k}) \right|^2 = \frac{1}{(2\pi)^2} \frac{2\pi D_K^2}{\sigma_m \omega_K} (1 - \cos \vartheta_{\mathbf{k}, \mathbf{k}'}), \quad (6)$$

where D_O is the optical phonon coupling constant, ω_O is the optical phonon frequency, D_K is the K -phonon coupling constant and ω_K is the K -phonon frequency. We denote by φ the sum of the angles $\vartheta_{\mathbf{k}, \mathbf{k}'-\mathbf{k}}$ and $\vartheta_{\mathbf{k}', \mathbf{k}-\mathbf{k}'}$, which are the convex angles between \mathbf{k} and $\mathbf{k}' - \mathbf{k}$ and between \mathbf{k}' and $\mathbf{k}' - \mathbf{k}$, respectively.

The presence of the SiO_2 substrate requires including also the interactions between the electrons of the graphene sheet and the remote phonons and impurities of the substrate. The remote optical phonons are assumed to have an energy equal to 55 meV and a deformation potential $D_f = 5.14 \times 10^7$ eV/cm. The electron-phonon scattering matrices have the same form as (4) and (5). Regarding the remote impurity scattering, we assume that they stay in a plane at distance d from the graphene sheet. The definition of the transition rate for electron-impurity scattering is highly complex; so many approximate models are proposed. We adopt the transition rate used in [3]

$$S^{(imp)}(\mathbf{k}, \mathbf{k}') = \frac{2\pi}{\hbar} \frac{n_i}{(2\pi)^2} \left| \frac{V_i(|\mathbf{k} - \mathbf{k}'|, d)}{\epsilon(|\mathbf{k} - \mathbf{k}'|)} \right|^2 \times \frac{(1 + \cos \vartheta_{\mathbf{k}, \mathbf{k}'})}{2} \delta(\varepsilon(\mathbf{k}') - \varepsilon(\mathbf{k})), \quad (7)$$

where

a) n_i is the number of impurities per unit area.

b) $V_i(|\mathbf{k} - \mathbf{k}'|, d) = 2\pi e^2 \frac{\exp(-d|\mathbf{k} - \mathbf{k}'|)}{\tilde{\kappa} |\mathbf{k} - \mathbf{k}'|}$,

- d is the location of the charged impurity measured from the graphene sheet
- $\tilde{\kappa}$ is the effective dielectric constant, defined by $4\pi\epsilon_0 (\kappa_{top} + \kappa_{bottom})/2$, where ϵ_0 is the vacuum dielectric constant and κ_{top} and κ_{bottom} are the relative dielectric constants of the medium above and below the graphene layer. In typical cases, the materials are SiO_2 and air, implying $\tilde{\kappa} = 4\pi\epsilon_0 (1 + \kappa_{\text{SiO}_2})/2 \approx 4\pi \times 2.45 \epsilon_0$.

c) the function $\epsilon(|\mathbf{k} - \mathbf{k}'|)$ is the 2D finite temperature static random phase approximation (RPA) dielectric (screening) function appropriate for graphene, and it is defined as follows

$$\epsilon(|\mathbf{k} - \mathbf{k}'|) = 1 + \frac{q_s}{|\mathbf{k} - \mathbf{k}'|} - \frac{\pi q_s}{8 k_F} \quad \text{if } |\mathbf{k} - \mathbf{k}'| < 2 k_F,$$

$$\epsilon(|\mathbf{k} - \mathbf{k}'|) = 1 + \frac{q_s}{|\mathbf{k} - \mathbf{k}'|} - \frac{q_s \sqrt{|\mathbf{k} - \mathbf{k}'|^2 - 4 k_F^2}}{2 |\mathbf{k} - \mathbf{k}'|^2} - \frac{q_s}{4 k_F} \text{asin} \left(\frac{2 k_F}{|\mathbf{k} - \mathbf{k}'|} \right) \quad \text{otherwise,}$$

- $q_s = (4 e^2 k_F) / (\tilde{\kappa} \hbar v_F)$ is the effective Thomas-Fermi wave-vector for graphene; it can be rewritten in terms of the dimensionless Wigner-Seitz radius as $q_s = 4 r_S k_F$; (we set $r_S = 0.8$)
- $k_F = \varepsilon_F / (\hbar v_F)$ is the Fermi wave-vector.

The physical parameters for the scattering rates are summarized in Table I. Some degree of uncertainty is still present

in the literature about the values of the scattering parameters [10]. However, our conclusions are quite independent on that.

TABLE I
 PHYSICAL PARAMETERS FOR THE SCATTERING RATES.

v_F	10^8 cm/s	v_p	2×10^6 cm/s
σ_m	7.6×10^{-8} g/cm ²	D_{ac}	6.8 eV
$\hbar \omega_O$	164.6 meV	D_O	10^9 eV/cm
$\hbar \omega_K$	124 meV	D_K	3.5×10^8 eV/cm
$\hbar \omega_{op-ac}$	55 meV	D_f	5.14×10^7 eV/cm

III. NUMERICAL RESULTS

The Boltzmann equation is discretized by using a DG approach. For the sake of brevity we skip the details about the numerical scheme; the interested reader is referred to [5]. Since only *electron dynamics in the conduction band of the valley K* is considered, the (conduction) electron density ρ and the (positive) Fermi energy ε_F are related by

$$\begin{aligned} \rho &= \frac{2}{(2\pi)^2} \int f(t, \mathbf{k}) d\mathbf{k} = \frac{2}{(2\pi)^2} \int f(0, \mathbf{k}) d\mathbf{k} \\ &= \frac{2}{(2\pi)^2} \int \frac{1}{1 + \exp\left(\frac{\varepsilon(\mathbf{k}) - \varepsilon_F}{k_B T}\right)} d\mathbf{k} \end{aligned} \quad (8)$$

which remains constant because the interband transitions can be neglected. We remark that the *total charge density* is equal to 2ρ , because we must also consider the equivalent valley K' .

We assume a lattice temperature T of 300 K, which will be kept constant. The surface impurity density n_i is set equal to 8.86×10^{11} cm⁻². The impurities are supposed to be distributed in a homogeneous way. A range from 0 to 1 nm is considered for the distance d between the graphene sheet and the remote impurities.

The simulations are performed at several values of the electric field and electron density. We take SiO₂ as substrate. The physical situation is schematically depicted in Fig. 1.

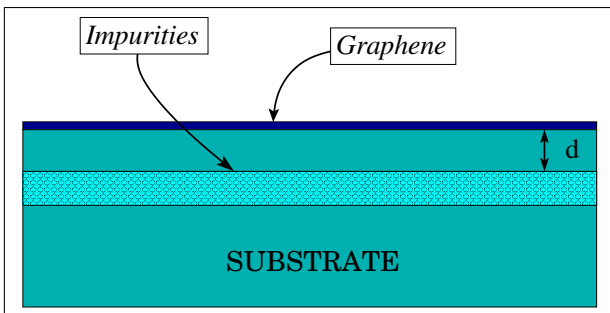


Fig. 1. The graphene sheet over a substrate.

In Fig. 2 and Fig. 3 the low field mobility (0.02 kV/cm) versus the electron density is reported for several values of the parameter d . The qualitative behavior, as regards the electron density, is similar to the expected one, see for example [1],

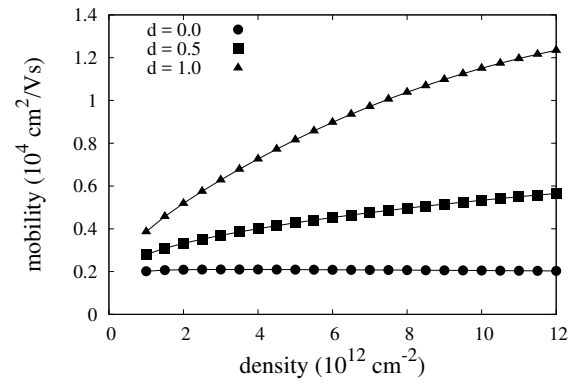


Fig. 2. Mobility for an electric field of 0.02kV/cm versus the electron density ρ for several values of the parameter d (in nm).

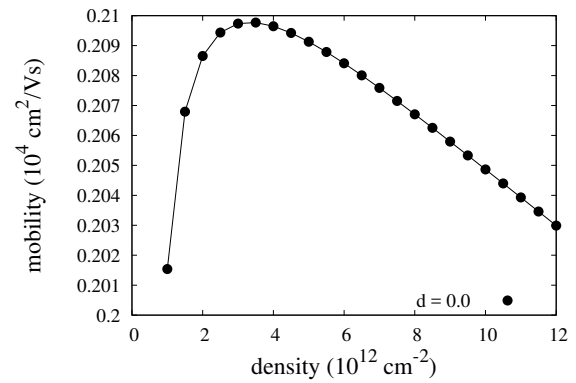


Fig. 3. Mobility for an electric field of 0.02kV/cm versus the electron density ρ in the case $d = 0$.

[2]. Our results clearly highlight a significant dependence of the mobility curves on the depth of the impurities inside the oxide. For small values of d one has an evident degradation of the mobility with respect to the suspended graphene case [11]. Therefore d is a relevant design parameter to be taken into account. For very small values of d ($d = 0$ in Fig. 3) there is a maximum of the low field mobility for an intermediate electron density, while it decreases for higher densities. For values around $d = 0.5$ nm, the low field mobility increases monotonically with the electron density. For higher values, about $d = 1$ nm, one recovers the mobility of the suspended case. To complete the analysis, in Figs. 4-5 there are plotted the mobility curves versus the electron density under an electric field of 10 kV/cm and 20 kV/cm, respectively. Again it is evident the strong influence of d . The qualitative dependence on the electron density is similar to the case of low field. As the electric field increases, the presence of a maximum value of the mobility for moderate doping is clearer and, of course for $d \approx 1$ nm we get the suspended case.

IV. CONCLUSIONS

Scattering between electrons and the remote impurities of the oxide is very important to determine the mobility curves

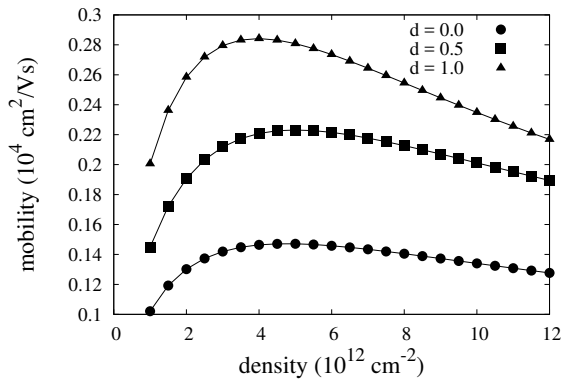


Fig. 4. Mobility for an electric field of 10 kV/cm versus the electron density ρ for several values of the parameter d (in nm).

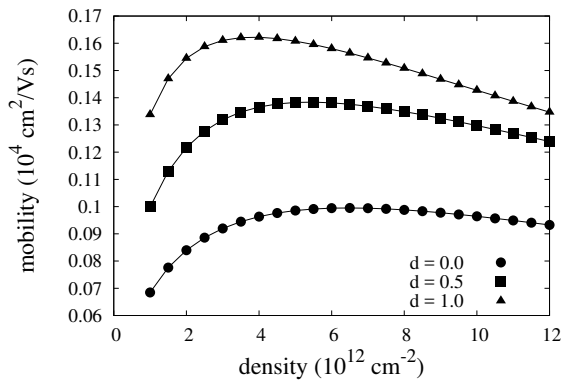


Fig. 5. Mobility for an electric field of 20 kV/cm versus the electron density ρ for several values of the parameter d (in nm).

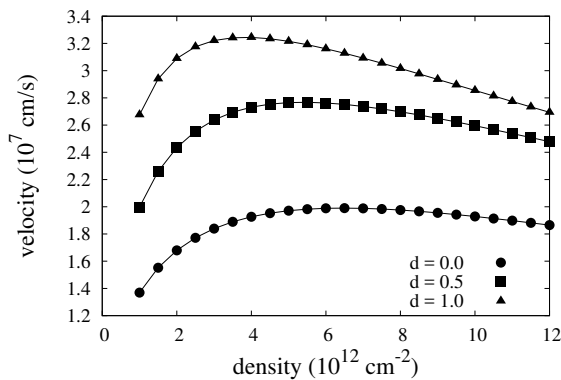


Fig. 6. Velocity for an electric field of 20 kV/cm versus the electron density ρ for several values of the parameter d (in nm) in the stationary regime.

in graphene on a substrate. In the models describing such an interaction, there is the presence of several parameters. In our analysis, by considering the dielectric function suggested in [3], it has been shown that a crucial parameter is the depth of the remote impurities with respect to the graphene layer. The statistical distribution of the impurity positions inside

the substrate is necessary for a correct determination of the mobility curves.

Several results are available in the literature but in the most part the dependence on d is ignored or it is not clear. The behavior of the velocity (Fig. 6, in the case $d = 0$) agrees with results obtained in [12] (Fig. 5) and differs from the data in [2], even if the discrepancy with this latter paper is not surprising, because we consider a simple sheet of graphene on SiO_2 with two (source and drain) contacts, while in ref. [2] a graphene ribbon with two additional gate contacts has been analyzed. We have also a good agreement with [1] (Fig. 5) for $d = 0$, while comparisons with [13]–[17] are difficult to perform and a certain degree of uncertainty still remains regarding the physical parameters and the dielectric function models.

ACKNOWLEDGMENTS

This work has been partially supported by the University of Catania, project F. I. R. *Charge transport in graphene and low dimensional systems*, and by INDAM (Istituto Nazionale di Alta Matematica).

REFERENCES

- [1] H. Hirai, H. Tsuchiya, Y. Kamakura, N. Mori and M. Ogawa, Electron mobility calculation for graphene on substrates, *J. Appl. Phys.*, vol. 116, 083703, 2014.
- [2] V. E. Dorgan, M. H. Bae and E. Pop, Mobility and saturation velocity in graphene on SiO_2 , *Appl. Phys. Lett.*, vol. 97, 082112, 2010.
- [3] E. H. Hwang and S. Das Sarma, Dielectric function, screening, and plasmon in two-dimensional graphene, *Phys. Rev. B*, vol. 75, 205418, 2007.
- [4] P. Lichtenberger, O. Morandi and F. Schürer, High-field transport and optical phonon scattering in graphene, *Phys. Rev. B*, vol. 84, 045406, 2011.
- [5] M. Coco, A. Majorana and V. Romano, Cross validation of discontinuous Galerkin method and Monte Carlo simulations of charge transport in graphene on substrate, *Ric. Mat.* DOI 10.1007/s11587-016-0298-4, 2016.
- [6] V. Romano, A. Majorana and M. Coco, DSMC method consistent with Pauli exclusion principle and comparison with deterministic solutions for charge transport in graphene, *J. Comput. Phys.*, vol. 302, pp. 267–284, 2015.
- [7] V. D. Camiola and V. Romano, Hydrodynamical model for charge transport in graphene, *J. Stat. Phys.*, vol. 157, 11141137, 2014.
- [8] G. Mascali and V. Romano, Charge transport in graphene including thermal effects, submitted to *Siam J. Appl. Math.*, 2016.
- [9] A. H. Castro Neto, F. Guinea, N. M. R. Peres, K. S. Novoselov, A. K. Geim, The electronic properties of graphene, *Rev. of Mod. Phys.*, vol. 81, pp. 109–162, 2009.
- [10] T. Fang, A. Konar, H. Xing and D. Jena, High-field transport in two-dimensional graphene, *Phys. Rev. B*, vol. 84, 125450, 2011.
- [11] A. Majorana, G. Mascali and V. Romano, Charge transport and mobility in monolayer graphene, submitted to *Journal of Mathematics in Industry*, 2016.
- [12] D. K. Ferry, Short-range potential scattering and its effect on graphene mobility, *J. Comp. Electronics*, vol. 12, pp. 76–84, 2013.
- [13] V. K. Arora, M. L. T. Tan and C. Gupta, High-field transport in a graphene nanolayer, *J. Appl. Phys.*, vol. 112, 114330, 2012.
- [14] A. Konar, T. Fang and D. Jena, Effect of high-k gate dielectrics on charge transport in graphene-based field effect transistors, *Phys. Rev. B*, vol. 82, 115452, 2010.
- [15] V. Perebeinos and P. Avouris, Inelastic scattering and current saturation in graphene, *Phys. Rev. B*, vol. 81, 195442, 2010.
- [16] R. Rengel, E. Pascual and M. J. Martin, Influence of the substrate on the diffusion coefficient and the momentum relaxation in graphene: the role of the surface polar phonons, *Appl. Phys. Lett.*, vol. 104, 233107, 2014.
- [17] A. Y. Serov, Z.-Y. Ong, M. Fischetti and E. Pop, Theoretical analysis of high-field transport in graphene on a substrate, *J. Appl. Phys.*, vol. 116, 034507, 2014.